

DOE/ET/20279--221

DOE/ET/20279-221

DE83 007476

Distribution Category UC 63a-e

**EFFECTS ON THE UTILITY FEEDER OF
UTILITY-INTERACTIVE INVERTERS AT THE NORTHEAST
RESIDENTIAL EXPERIMENT STATION**

P.S. Shelton, Consultant

F.J. Solman

B.E. Nichols

January 1983

DISCLAIMER

This report was prepared as an account of work sponsored by an agency of the United States Government. Neither the United States Government nor any agency thereof, nor any of their employees, makes any warranty, express or implied, or assumes any legal liability or responsibility for the accuracy, completeness, or usefulness of any information, apparatus, product, or process disclosed, or represents that its use would not infringe privately owned rights. Reference herein to any specific commercial product, process, or service by trade name, trademark, manufacturer, or otherwise does not necessarily constitute or imply its endorsement, recommendation, or favoring by the United States Government or any agency thereof. The views and opinions of authors expressed herein do not necessarily state or reflect those of the United States Government or any agency thereof.

NOTICE

**PORTIONS OF THIS REPORT ARE ILLEGIBLE. It
has been reproduced from the best available
copy to permit the broadest possible avail-
ability.**

Prepared for

THE U.S. DEPARTMENT OF ENERGY

UNDER CONTRACT NO. DE-AC02-76ET-20279

MASTER

DISCLAIMER

This report was prepared as an account of work sponsored by an agency of the United States Government. Neither the United States Government nor any agency thereof, nor any of their employees, makes any warranty, express or implied, or assumes any legal liability or responsibility for the accuracy, completeness, or usefulness of any information, apparatus, product, or process disclosed, or represents that its use would not infringe privately owned rights. Reference herein to any specific commercial product, process, or service by trade name, trademark, manufacturer, or otherwise does not necessarily constitute or imply its endorsement, recommendation, or favoring by the United States Government or any agency thereof. The views and opinions of authors expressed herein do not necessarily state or reflect those of the United States Government or any agency thereof.

DISCLAIMER

Portions of this document may be illegible in electronic image products. Images are produced from the best available original document.

Blank Page

ABSTRACT

The utility feeder for the Northeast Residential Experiment Station (NE RES) in Concord, MA, is a 2.4/4.16-kV circuit from the Concord Municipal Light Plant. The line was modeled analytically to predict the effects of loads and injected photovoltaic (PV) power applied at the NE RES. Measurements were made with instrumentation installed on the feeder near the substation and at the NE RES. The effects were compared with predictions. Measurements of ambient harmonic voltage and currents were made near the substation.

Blank Page

TABLE OF CONTENTS

<u>Section</u>		<u>Page</u>
	Abstract	iii
	List of Figures	vi
	List of Tables	vii
1.0	INTRODUCTION	1
2.0	LOCATION OF STUDY	2
3.0	MODELING PROCEDURES	3
	3.1 Load Model	3
	3.2 High-Voltage Line Model	6
4.0	CALCULATED RESULTS FROM MODELS	9
	4.1 Feeder Voltage Profiles	9
	4.2 Line Loss Reduction with PV Generation	10
	4.3 Effect of Power Factor on Line Voltage	13
	4.4 VAR Demand and Power Factor	14
	4.5 Distribution Transformer and Low-Voltage Wiring	15
	4.6 Effect of Inverter Harmonics	17
	4.6.1 Harmonic Effects on High-Voltage Line	18
	4.6.2 Harmonic Effects on Transformer and Secondary	19
5.0	UTILITY FEEDER INSTRUMENTATION	21
6.0	COMPARISON OF MODEL PREDICTIONS WITH MEASUREMENTS	25
	6.1 Loading Tests at NE RES	25
	6.2 PV Injection from the NE RES	26
7.0	MEASUREMENT OF AMBIENT HARMONIC VOLTAGES AND CURRENTS	29
8.0	CONCLUSIONS	31
	References	32
	Appendix A - Line Losses Versus Load and PV Injection	

LIST OF FIGURES

<u>Figure</u>		<u>Page</u>
1	Map of Concord Municipal Light Plant (Circuit 23).	4
2	Line and load model of CMLP Circuit 23.	7
3	Simplified model of CMLP Circuit 23.	7
4	Simplified network model of CMLP Circuit 23 at 60 Hz.	8
5	Voltage profile of CMLP Circuit 23 with typical summer loads.	9
6	Voltage change with injection of 500 kW of PV generation at NE RES on CMLP Circuit 23.	10
7	Relation of voltage fluctuation tolerance to frequency of occurrence (incandescent lamps).	11
8	Vector diagram for injected current on a feeder.	13
9	Typical distribution transformer and low-voltage secondary circuit.	16
10	Simplified network for calculating current division at fundamental and harmonics.	18
11	(a) Pole-top-mounted transformers for UDAC; (b) UDAC block diagram.	22
12	Feeder measurements with switched loads at NE RES.	27
13	Feeder measurements with PV-generated power injected at NE RES.	28
14	Voltage and current waveforms measured on CMLP Circuit 23 at Pole 17.	29

LIST OF TABLES

<u>Table</u>		<u>Page</u>
I	(a) Concord Municipal Light Plant Circuit 23 Conductor Characteristics; (b) Line Lengths, Line Impedance and Estimated Loads for Concord Municipal Light Plant Circuit 23	5
II	Line Loss Reduction with PV Generators on CMLP Circuit 23	12
III	Inverter Power Factors for Minimum Voltage Change as a Function of Primary Conductor Size	14
IV	Distribution Transformer and Secondary Circuit Impedances	16
V	Current Division at Fundamental and Harmonics for 500 kW of Power Injected at the End of Circuit 23	18
VI	Sources of Capacitor Current at Fundamental and Harmonics with Power Injected at End of Circuit 23	19
VII	Summary of UDAC Instrumentation Capabilities	23
VIII	Daily Summary from UDAC Measurements	24
IX	Harmonics Measured on CMLP Circuit 23 at Pole 17 (May 14, 1982 between 2 and 4 p.m.)	29

1.0 INTRODUCTION

The purpose of the work which this report describes was to form a basis and methodology for predicting the effect of photovoltaic (PV) generation on utility distribution systems, and to determine, if practicable, the required design parameters and limitations on the quantity and size of such sources. The methods were applied to a case study of a feeder serving the PV systems at the Northeast Residential Experiment Station in Concord, Massachusetts, and were verified by experimental measurements where possible.

The need for this study arose because electrical distribution systems are increasingly required to operate in modes for which they were not originally designed (1). Electrical distribution feeders have typically operated in a radial, unidirectional mode with a source at the substation end, and loads either distributed along the feeder or concentrated at the other end.* Occasional sources of parallel generation were handled as specific design problems.

The principal emphasis of this report is on PV generation effects on the high-voltage (primary) lines between the substation and the distribution transformers. Problems in this portion of the distribution system affect larger numbers of customers and the circuitry cannot be easily changed. As is shown later in this report, voltage changes in the distribution transformer and secondary (120/240 volt) wires are generally only a few percent, or can be reduced to a small number by simple changes in secondary wiring or by adding a transformer.

*In some high-density urban areas, dual or network feeds of a utility distribution feeder are in use. By energizing the distribution feeder from substations at each end, higher service reliability is often possible as well as reduced voltage variations with load changes. This kind of feeder was not analyzed in this study.

2.0 LOCATION OF STUDY

The feeder studied is part of the Concord Municipal Light Plant (CMLP) system located in Concord, Massachusetts. Interconnected with this feeder is MIT Lincoln Laboratory's Northeast Residential Experiment Station (NE RES), which presently contains five PV-generating sources, all of which operate in parallel with the utility.

This particular combination of feeder and PV system is uniquely suitable for study of the PV-utility interrelationship. The feeder is relatively small (2 MW) and electrically limber. It operates at a relatively low voltage (2400/4160 volts), making observation and measurement of phenomena comparatively simple. The NE RES, located at the end of the feeder about three miles from the substation, is highly instrumented and well-equipped to monitor and record the required data (2). The instrumentation of the feeder is discussed in a later section of this report.

3.0 MODELING PROCEDURE

Concord Municipal Feeder 23 (Fig. 1 and Table Ia and b) is a 2400/4160 volt, three-phase, 4-wire feeder with approximately three miles of 1/0 copper main line, and several additional miles of single- and three-phase branches. The feeder is fed from a six-feeder, double-ended bus at Substation 341 located on Walden Street, Concord. The feeder has a bank of three 100-kVAR capacitors located near the junction of Old Bedford Road and Virginia Road, and three single-phase line regulators about halfway out Virginia Road. The NE RES is located at the far end of the feeder, along with several large commercial loads.

Conventional distribution-feeder-modeling techniques were modified to permit modeling the effects of injected power from PV sources at locations other than the primary source at the substation. While fundamental frequency power injection might properly be treated as a negative load, the need to analyze harmonic effects requires a more adaptable model. A network configuration was adopted which is capable of current injection at any of several points. The net effect of multiple sources and loads was solved by superposition.

3.1 Load Model

In order to simplify model configuration as much as possible, the feeder loads were lumped at various points along the feeders.

Since most utilities, including this one, devote considerable effort to keeping their distribution transformers properly sized for the load they must carry, distribution transformer locations and sizes provide a reasonably good basis for estimating load distribution. For modeling this feeder, the load at each point (or bus) was estimated by apportioning the total feeder load in direct proportion to the connected distribution transformer kVA.

Net feeder load (including power-factor-correction capacitor banks), as seen at the substation, was estimated by CMLP to be approximately 1900 kVA on summer peak at 0.90 power factor, and at about 1500 kVA on a typical summer day. In complex notation, net values of $1710 - j828$ kVA were used to represent the peak load with an additional 300-kVA reactive assumed to be furnished

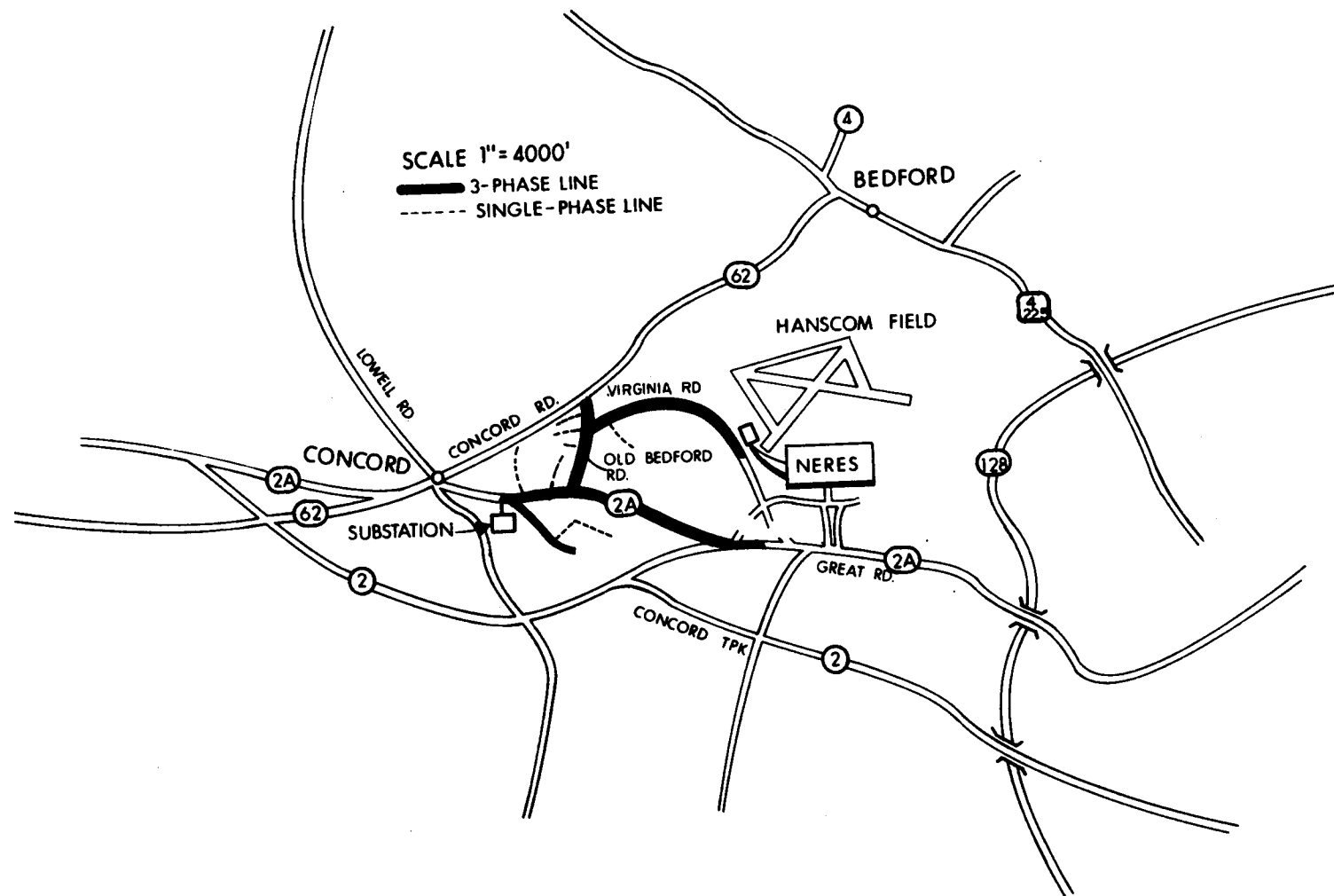


Fig. 1. Map of Concord Municipal Light Plant (Circuit 23).

TABLE Ia
CONCORD MUNICIPAL LIGHT PLANT CIRCUIT 23 CONDUCTOR CHARACTERISTICS

3 1/0 cu. conductors - spacing 72" x 14" x 86" = 44.25" equiv.

R = .105 ohms/1000'

X₁ = .1035 ohms/1000'

X₂ = .03 ohms/1000'

Total X = .1335 ohms/1000'*

Z₁ = .105 + j.1335 ohms per thousand feet

Neutral = 1/0 alum. in parallel with 052 AWA messenger (est.)

1/0 alum. = .16 ohms/1000'

052 AWA = .179 ohms/1000'

Both = .0844 ohms/1000'

Plus 1/0 cu. phase wire = .105 ohms

R_o = .0844 + .105 = .189 ohms/1000' single phase R

X_o = $\frac{X_1}{2} + X_2 + (X_1 + X_2) = 0.215 \text{ ohms/1000'}$

Z_o = .189 + j.215 ohms/per thousand feet

Feeder has 1-300 kVAR 3-phase fixed capacitor at about midpoint.

Feeder has 3-10% single-phase line regulators 3000' from load end.

Substation power transformer = 6.04% Z on 7500 kVA base.

Z_t (ohms) = 6.04% x 10 (17.3)/7500 = j.139 ohms

Substation getaway cable = 350 MCM x 600' = (.043 + j.07) x .6
(from substation bus to overhead wires) = .026 + j.04

*Data from Reference 3.

TABLE Ib
LINE LENGTHS, LINE IMPEDANCE AND ESTIMATED LOADS FOR
CONCORD MUNICIPAL LIGHT PLANT CIRCUIT 23

Section	Length	Conductor	Line Z ₁	Connected Transformer kVA	Estimated** Tapped Load (kVA)	Amperes
0-1	500'	3-350 MCM***	.026+j.179	392.5	168-j102	23-j14
1-2	1600'	3-1/0 cu.	.168+j.214	315	135-j82	19-j11
2-3	1000'	"	.105+j.134	242.5	104-j63	14-j9
3-4	2600'	"	.273+j.347	414	178-j108	25-j15
4-5	1600'	"	.168+j.214	232.5	100-j60	14-j8
5-6	1200'	"	.126+j.160	87.5+300 cap	38+j277	5+j39
6-7	1000'	"	.105+j.134	360	155-j94	22-j13
7-8	3000'	"	.315+j.401	3-1 ph. 10% regulators		
8-9	3000'	"	.315+j.401	1965	845-j511	117-j71
			1.601+j2.84		1723-j743	

**Loading was estimated by proportioning connected distribution transformer kVA to feeder peak kW and kVAR.

***MCM = thousands of circular mils.

by the capacitor, giving a raw load of $1710 - j1128$ kVA to be apportioned over the feeder. For calculations at other feeder loads, a load power factor between 0.86 and 0.90 was assumed and a similar procedure was used.

The presence of large commercial loads which may peak at times different from the residential load could introduce a potential source of inaccuracy, since it changes the distribution of load on the feeder. Such loads are present on the subject feeder, but the degree of inaccuracy was not considered to be significant in the context of the objectives of this study.

3.2 High-Voltage Line Model

Line characteristics were derived by methods described in Chapter 1 of the GE Distribution Data Book (3). Each of three 1/0 copper conductors with spacings of 72 in. \times 14 in. \times 86 in. (44.25 in. equivalent) are calculated to have resistance equal to 0.105 ohms per 1000 feet and reactance equal to $+j0.1335$ ohms per 1000 feet. These values represent the impedance of one phase of a balanced three-phase line.

Because loading and solar injection at the NE RES are arranged on a single-phase basis and connected from phase to neutral, Z_o , or single-phase impedance, was also calculated. This required adding neutral impedance for a neutral conductor system consisting of one 1/0 aluminum conductor in parallel with an Alumoweld spacer cable messenger, and in further parallel with earth, since both neutrals are grounded throughout their length. Z_o is calculated at $0.189 + j0.215$ ohms per 1000 feet, with some probable but indeterminate reduction due to parallel ground-path conductance.

Figure 2 represents the main line of the feeder with the loads grouped as described above. Loads at each bus are shown as connected transformer kVA, apportioned load kVA in complex notation, and three-phase amperes in complex notation. Line sections between buses are shown as distances in feet, and in ohms impedance on a balanced three-phase basis. This model was analyzed by a computer model developed by Fitzer (4) as well as by simplified models described below.

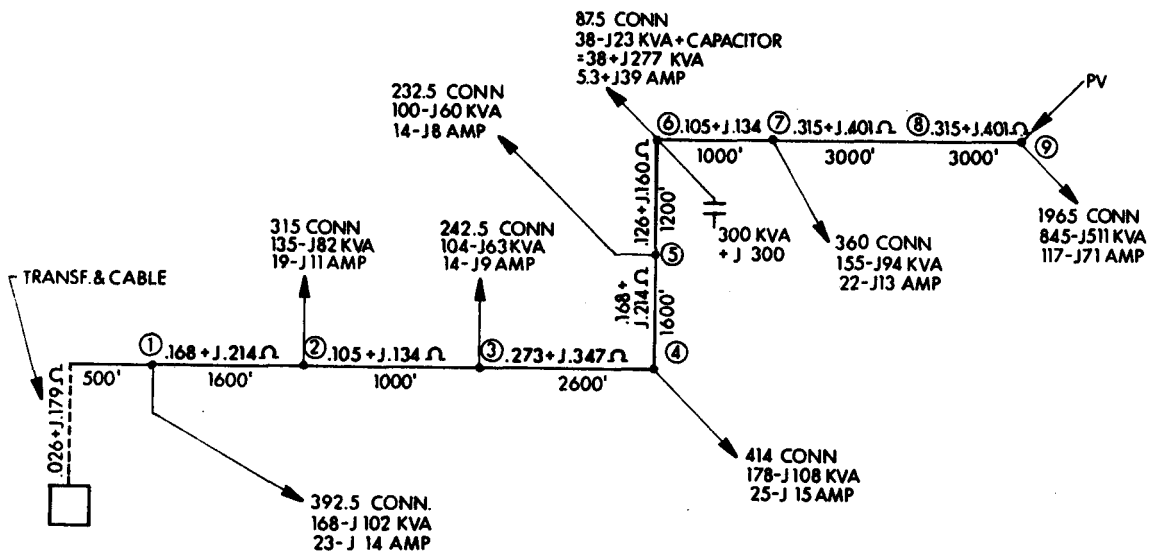


Fig. 2. Line and load model of CMLP Circuit 23.

The network resulting from Fig. 2 was further simplified to the equivalent circuit shown in Fig. 3.

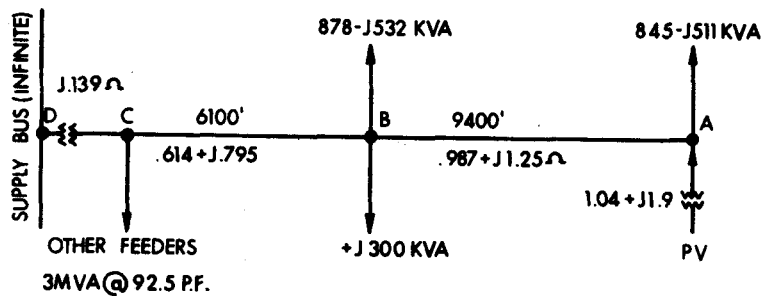


Fig. 3. Simplified model of CMLP Circuit 23 at 60 Hz.

This was then converted into an impedance network (Fig. 4), which could be fed from either end, with the utility high-tension system acting essentially as a transformer impedance limited short circuit when the network is fed from the NE RES (PV) end.

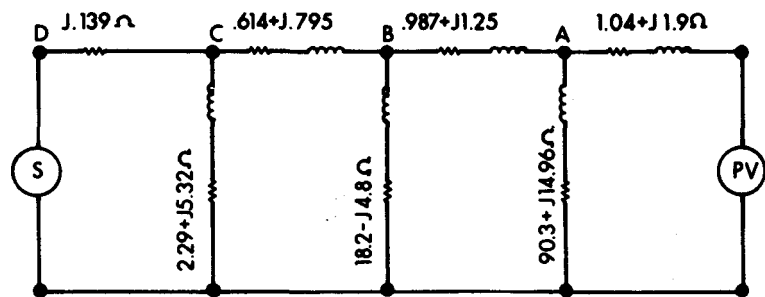


Fig. 4. Simplified network model of CMLP Circuit 23 at 60 Hz.

For harmonic analysis, the line and load inductive and capacitive reactances are adjusted to correspond with the harmonic frequency when harmonic currents are injected from the NE RES end (5).

4.0 CALCULATED RESULTS FROM MODELS

4.1 Feeder Voltage Profiles

A set of voltage profiles for the Concord feeder (Fig. 5) was drawn from computer runs made by Fitzer at the University of Texas, using load and impedance data for the model represented by Fig. 2. These profiles show minimal voltage variation resulting from injection of presently available amounts of PV power at the NE RES. Note that the substation load is reduced by more than the amount of solar generation. This is discussed in the next section.

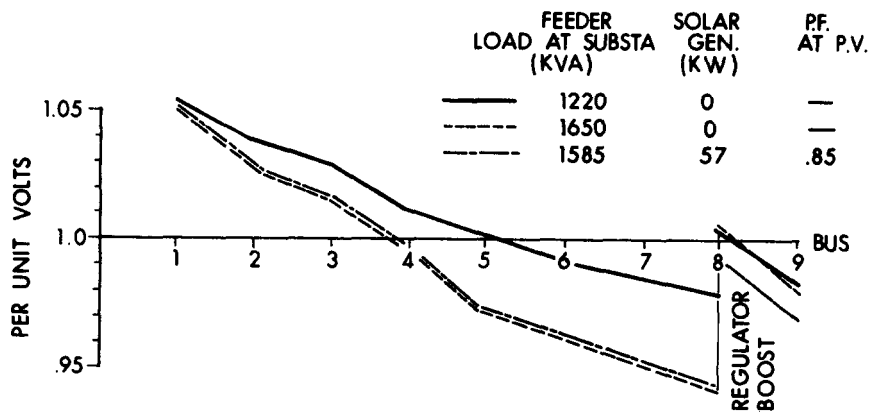


Fig. 5. Voltage profile of CMLP Circuit 23 with typical summer loads.

Since the effect on voltage would appear to be a limiting factor in the application of PV generation, the calculations were expanded to encompass arbitrary injection of 500 kW of PV generation (more than 25% of the feeder rating) at various power factors and at various load levels.

Voltage drops were calculated for two levels of feeder loading, for conditions of no PV generation, and for injection of 500 kW of PV generation at three different injection power factors. Results of these calculations are shown graphically in Fig. 6. Note that for a PV inverter power factor of 0.78 there is no change in voltage. This "no boost" power factor will be explained in the section dealing with the effects of power factor on line voltage.

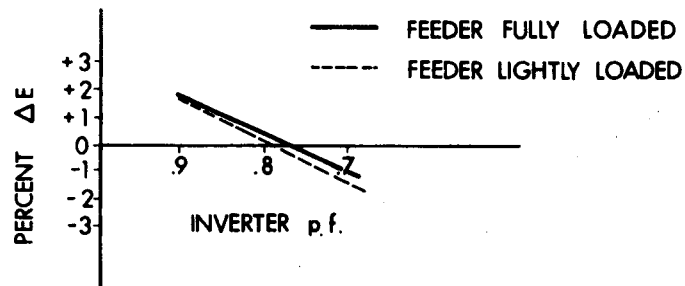


Fig. 6. Voltage change with injection of 500 kW of PV generation at the NE RES on CMLP Circuit 23.

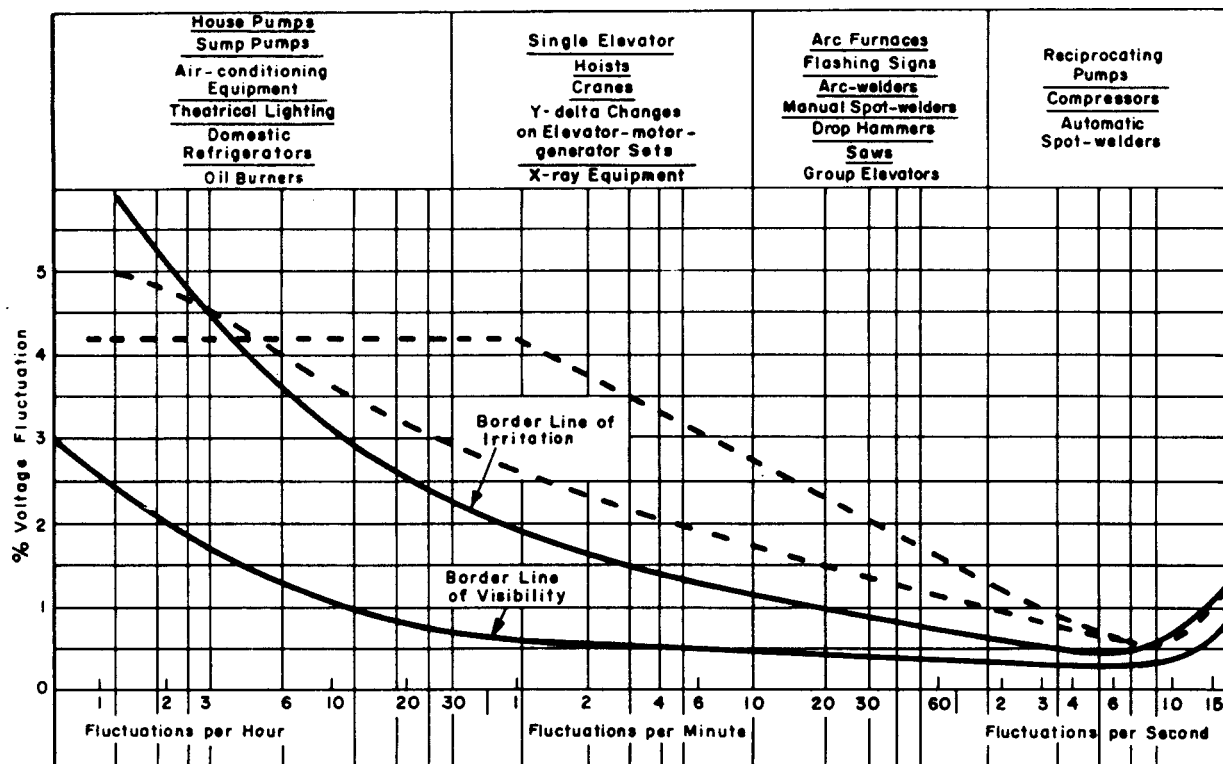
It was assumed that the limiting characteristic would be the voltage fluctuation occurring with rapid changes in insolation. Assuming as a worst case all of the PV generation at a single location, and a maximum variation from 500 kW to 0, the maximum voltage change is seen to be about 1.5% at 0.9 PF.

Reference to industry-recognized criteria for voltage fluctuation (Fig. 7) suggests that this value is quite tolerable up to frequencies of two per minute. Further, since the insolation-controlled change in voltage would not be instantaneous, it is expected that larger changes could be tolerated.

These predictions were based on the assumption that the power factor of the inverter output remains approximately constant over the expected range of injection levels, which is consistent with performance of presently available equipment. Deterioration of power factor with decreasing power would increase the resulting voltage change. Further study may be necessary to define these limits precisely.

4.2 Line Loss Reduction with PV Generation

Significant savings can be realized in the operation of a distribution feeder with PV generation by reducing line losses. This is particularly true of the Concord Feeder 23 in view of the heavy loading, the low design voltage (2400/4160 V) and the small wire size. Since line losses vary as the square of the line current, application of even small amounts of solar generation near the end of a heavily loaded feeder can have a significant effect on the amount of power supplied by the utility at the substation end.



Solid Lines composite curves of voltage flicker studies by General Electric Company, *General Electric Review* August 1925; Kansas City Power & Light Company, *Electrical World*, May 19, 1934; T. & D. Committee, EEI, October 24, 1934, Chicago; Detroit Edison Company; West Pennsylvania Power Company; Public Service Company of Northern Illinois.

Dotted Lines voltage flicker allowed by two utilities, references *Electrical World* November 3, 1958 and June 26, 1961.

Fig. 7. Relation of voltage fluctuation tolerance to frequency of occurrence (incandescent bulbs) (3).

Table II shows the results of a computer simulation of CMLP Circuit 23 with a very heavy load on the circuit. The base case of a load of 2089 kW at the substation is compared with 50 kW of PV injection at three power factors. The PV power is assumed to be injected at the end of the feeder at the NE RES. Note that the change in power at the substation is larger than the amount of PV power injected. This is due to the reduction in line current and hence the I^2R losses. The ratio of power reduction at the substation divided by PV power injected is expressed as the percentage labeled "solar bonus." For PV injection of 50 kW at unity power factor, the load at the substation is reduced 67 kW. The substation has to supply 17 kW less power, which is a bonus benefit of an additional 34%.

TABLE II
LINE LOSS REDUCTION WITH PV GENERATION AT NE RES
HEAVY LOAD ON CMLP CIRCUIT 23

Condition	Power from sub-station in kW	$\Delta P_{\text{substation}}$ kW	Line Losses in kW	as % of Load	Δ Loss in kW	P_{solar} kW	Solar Bonus %
No PV generation:	2089	--	218	11.7	--	0	--
50-kW PV generation: PF = 1.0	2022	67	201	11.0	17	50	34
50-kW PV generation: PF = 0.85	2028	60	208	11.4	11	50	21
50-kW PV generation: PF = 0.7	2033	56	212	11.6	6	50	12

$$\text{Solar Bonus} = \left(100 \times \frac{\Delta P_{\text{substation}}}{P_{\text{solar}}} \right) - 100$$

The effect of inverter power factor on solar bonus is most significant on a feeder heavily loaded in relation to its capacity. Table II and Appendix A show that the reduction in substation load is less with lower inverter power factors. The difference in solar bonus for a unity power factor inverter versus 0.85 power factor ranges from about 13% in the heavily loaded case shown in Table II to about 1% for the low-line-loss Texas Electric Service Company (TESCO) feeder discussed in Appendix A. As line losses increase, the PV bonus benefit is greater, since transmission losses become a larger proportion of the power that must be supplied by the utility.

This phenomenon has been discussed by Fitzer (4) but it was less dramatic (about 3%) for the feeder he studied since that feeder operated at a higher voltage (7.2/12.5 kV) and line losses were lower.

4.3 Effect of Inverter Power Factor on Line Voltage

It can be shown by using the line impedance values in the model that at inverter power factors in the order of 0.75 to 0.80 the voltage rise in the feeder produced by the in-phase component of the injected power approximately equals the voltage drop caused by the reactive component (Fig. 8). The amount of injected kVA has little if any effect on the customer's voltage at any point on the feeder. Because of this, flicker due to insolation changes should be minimal for inverters operating at the power factors mentioned above.

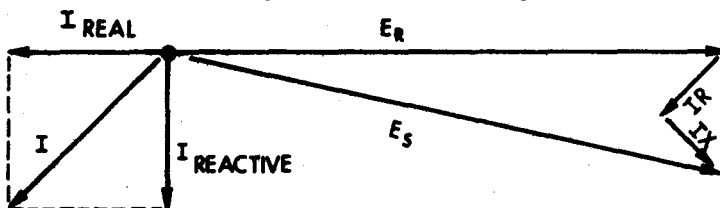


Fig. 8. Vector diagram for injected current on a feeder.

The inverter power factor value at which this condition is true may vary from feeder to feeder. It can be shown that the "non-boost" inverter power factor is actually a function of the R/X ratio of the particular circuit involved. The conventional approximation for voltage drop:

$$\Delta E = I (R \cos \theta + X \sin \theta)$$

can be modified to reflect the negative value of the in-phase inverter current (PV power). If ΔE is the voltage change produced at the point of PV power injection, then:

$$\Delta E = -I_{inv} R \cos \theta + I_{inv} X \sin \theta.$$

As ΔE reaches minimum value:

$$0 = -I_{inv} R \cos \theta + I_{inv} X \sin \theta$$

$$I R \cos \theta = I X \sin \theta$$

$$\frac{R}{X} = \frac{\sin \theta}{\cos \theta} = \tan \theta.$$

Therefore, for any particular circuit the tangent of the non-boost inverter power factor angle will equal the R/X ratio of the feeder from its source to the point of injection. Non-boost inverter power factors for several conductor sizes are tabulated in Table III.

TABLE III
INVERTER POWER FACTORS FOR MINIMUM VOLTAGE CHANGE AS A FUNCTION
OF PRIMARY CONDUCTOR SIZE

<u>Conductor</u>	<u>Inverter PF for Minimum ΔE</u>
477 MCM Alum.*	0.95
336 MCM Alum.	0.91
4/0 Alum.	0.83
1/0 Alum.	0.62
1/0 Copper	0.78
4 Copper	0.48

4.4 VAR Demand and Power Factor

The inadequacy of defining power factor of any utility-interactive energy source is discussed by Campen (6). She correctly establishes that power factor alone is a misleading measure of the interconnection. This can easily be seen by considering the case when the real power generated by a

* 477 MCM Aluminum wire has a cross section area of 477,000 circular mils.

residential PV inverter exactly equals the real power consumed by the house load. When this occurs, the power factor is zero if any reactive load is present. The true measure of the effect of any positive or negative load on the utility is best expressed in terms of the VAR* demand of the load. Reactive power is a load which must be supplied by the interconnected system just as must real power.

In Section 4.3 it was shown that inverters that operate at less than unity power factor can have minimal impact on feeder voltage. The net VAR load which this creates must be supplied in some manner. To supply it in conjunction with and at the point of PV injection obviously defeats the voltage regulation benefit and would result in a voltage boost as power injection is increased.

Most utilities design their distribution and supply systems to operate at or close to zero reactive factor. This is generally accomplished by combinations of fixed and switched capacitors at points near the load centers of the feeders. It seems obvious that these installations must be augmented to supply the reactive requirements of a substantial quantity of PV inverters. In addition, more exotic control devices than the common time switches or current controls will be needed, due to the time uncertainties of PV insolation.

4.5 Distribution Transformer and Low-Voltage Wiring

Figure 9 shows a typical neighborhood cluster of houses served from a distribution transformer. The sizing of the transformer and wire is representative of current practice in the New England region and assumes normal diversity and transformer overload capability. The design load for each house is about 5 kW and is typical for houses without electric space heating.

* VAR = volt amperes reactive, or reactive power.

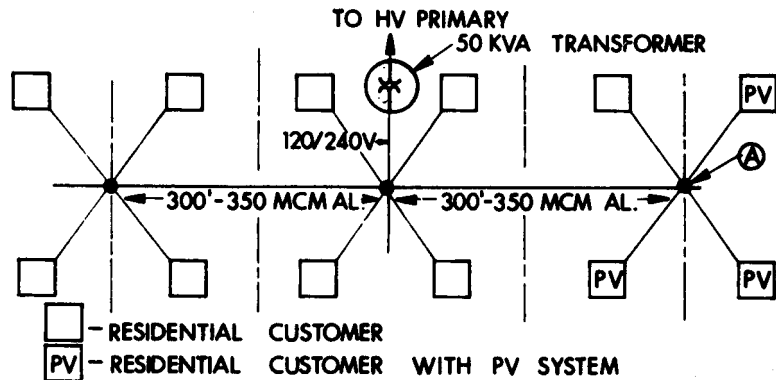


Fig. 9. Typical distribution transformer and low-voltage secondary circuit.

Table IV shows a summary of the impedances at the fundamental and harmonic frequencies. Harmonic impedances were calculated from the 60-Hz impedance by increasing the inductive reactance in proportion to the frequency of the harmonic. Harmonics currents are from Landsman (7).

Using the values from Table IV, voltage drop with 20 kW of load (240 V) at Point A on Fig. 9 is about 2%. (Some additional voltage drop will occur in the service drop from Point A to the house distribution panel but will affect only that particular house.)

TABLE IV
DISTRIBUTION TRANSFORMER AND SECONDARY CIRCUIT IMPEDANCES

50 kVA transformer:	0.0127 + j 0.0208
350 MCM Triplex cable: 300' span	0.034 + j 0.016
Total source impedance at Point A	0.0467 + j 0.0368
Assumed impedance at 3rd harmonic:	0.0467 + j 0.1104 ; Z = 0.1198
5th harmonic:	0.0467 + j 0.184 ; Z = 0.1898
Assumed harmonic current at 3rd harmonic:	4.5 amperes x 3 = 13.5 amperes
5th harmonic:	1.5 amperes x 3 = 4.5 amperes
Harmonic voltage seen at Point A (on 240 V basis)	
3rd harmonic:	1.61 V (0.6%)
5th harmonic:	0.85 V (0.35%)

Reference: GE Distribution Data Book (3)

In addition to the configuration shown in Fig. 9, several other common sizes and configurations of secondary (120/240 V, single-phase) circuit were examined. The 300-foot run using two common sizes of underground or overhead cable and two common sizes of open wire secondary was analyzed for voltage change (ΔE) resulting from injection of 18 kW (3 units of 6 kW each) of PV generation at 0.80 power factor. The results are tabulated below. These values include the voltage change through the 50-kVA distribution transformer.

<u>Size and Configuration</u>	<u>ΔE @ 0.80 PF</u>	<u>Nonboost PF</u>
3/0 cable	-1.7%	0.41
350 MCM cable	-0.6%	0.61
1/0 open wire	-1.6%	0.59
4/0 open wire	-0.16%	0.78

4.6 Effect of Inverter Harmonics

The harmonic currents reported by E. E. Landsman (7) from measurements on a line-commutated inverter were used as a basis for the analysis. In this type of inverter only the 3rd, 5th and 7th harmonics of 60 Hz are of significant amplitude. Higher harmonics exist but these are of even smaller magnitude and can easily be filtered. This power converter probably represents a "worst case" for harmonic generation and power factor. (A harmonic filter and power-factor correction for this type of inverter, which significantly reduces harmonic currents, has been tested. It is unlikely that significant numbers of this kind of worst-case unit would be installed.)

Landsman's work suggests values for a line-commutated inverter without filtering of 4.5 amperes of 3rd harmonic current and 1.5 amperes of 5th for 5 kW of solar generation at 240 volts. Expanding these values for 500 kW of solar (166 kW per phase on a 2400/4160-V, three-phase line) gives currents of 15 amperes of 3rd and 5 amperes of 5th, if all inverters add their harmonic content in the same time/phase relationship. To calculate the effects of harmonic currents, the approximation was made that the inductors represented in the models for the line and loads from Figs. 3 and 4 could be scaled and that the system capacitor bank reactances could also be scaled. Figure 10 and Table V show how the injected current divides.

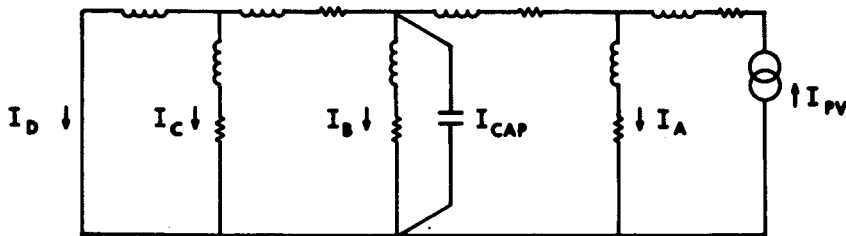


Fig. 10. Simplified network for calculating current division at fundamental and harmonics.

TABLE V
CURRENT DIVISION AT FUNDAMENTAL AND HARMONICS
FOR 500 kW AT POWER INJECTED AT THE END OF CIRCUIT 23

Path	Harmonic: Frequency:	1 60 Hz amperes	3 180 Hz amperes	5 300 Hz amperes
I_A (nearby loads)		12.0 (14)*	2.3 (15)	0.6 (11)
I_B (other loads)		9.0 (11)	2.2 (15)	0.4 (9)
I_C (other feeders on same bus)		13.0 (16)	2.3 (15)	0.6 (12)
I_D (HV distribution system)		45.0 (54)	4.2 (28)	0.7 (13)
I_{cap} (300-kVAR capacitor)		4.0 (5)	4.0 (27)	2.7 (55)
Total Injected Current		83.0	15.0	5.0

*Values in () are percent of total injected current.

4.6.1 Harmonic Effects on High-Voltage Line

Table VI shows the sources and values of the capacitor current. It would appear from these values that in the specific case of the Concord feeder, 4 amperes of 3rd harmonic and 2.75 amperes of 5th find their way to the capacitor. Since capacitors are designed to handle combined fundamental and harmonic currents up to 135% of their rating (8), this provides an overload margin of

14.5 amperes. It is concluded that no problem would be created, particularly since at this level of generation, additional capacitors would be desirable for system power factor correction, thus providing additional harmonic sink capability.

TABLE VI

SOURCES OF CAPACITOR CURRENT AT FUNDAMENTAL
AND HARMONICS WITH 500 kW OF POWER INJECTED AT THE END OF CIRCUIT 23

Frequency (Harmonic)	Due to Feeder amperes	Due to Injected Power amperes	Total Per Phase amperes
60 Hz (1)	--	--	41.67
180 Hz (3)	0.88	4.00	4.88
300 Hz (5)	2.71	2.75	5.46
420 Hz (7)	0.73	2.00	2.73
	4.32	8.75	54.74

1. Currents due to feeder were calculated assuming the naturally occurring harmonic voltage measured on A phase (Table IX) was present at the capacitor bank.
2. The current output spectrum for 500 kW of PV injection was obtained from Landsman's report (7) for a line-commutated inverter. It is a worst case as inverters under current development have less distortion.
3. Total current per harmonic is obtained by adding currents due to harmonics voltages on feeder to the current due to the injected power. This is a worst case since they may not all add in phase. All currents shown are RMS.

4.6.2 Harmonic Effects on Transformer and Secondary

In order to examine the effect of harmonic current injection at the secondary level, the model of representative residential secondary layout (see Fig. 9 and Table IV) was used. A secondary circuit of 12 houses requiring approximately 5 kW each is assumed to be fed from a 50-kVA transformer over 350-MCM aluminum triplex cable. Based on a 25% PV saturation, we have assumed a "worst-case" condition placing all three PV units at one end of the secondary circuit.

Using harmonic currents described previously, harmonic voltages of 0.6% for 3rd harmonic and 0.35% for the 5th are calculated. These values are well within the levels already existing on the feeder, and would not appear to be harmful (see Table IV).

Some additional voltage would appear across the primary circuit (depending on the location on the feeder and the distances to the substation and to other harmonic sinks, such as capacitors), but is not expected to be significant, particularly since a multiplicity of such installations would be balanced on the three-phase feeder.

5.0 UTILITY FEEDER INSTRUMENTATION

One of the special features of the Concord feeder installation is a load-information-gathering and recording system. This system, described by Fenton and Much (2), was expanded to record information about the feeder itself. A utility-data-acquisition unit (UDAC) was installed as close to the substation end of the feeder as was practical, and another was placed at the NE RES location at the load end. (A third similar unit monitors a feeder from Boston Edison's Lexington substation for load studies.)

It was not possible to locate the source-end unit in the substation because of space and operational concerns, but space was available on Pole 17 on Lexington Road, Concord, just beyond the feeder riser. Construction was such that one branch of the feeder (node 1) tapped off ahead of the sensor, but this was not considered to be of major significance.

These installations collect and transmit to the data system at the NE RES the following data pertinent to both source and load ends of the feeder:

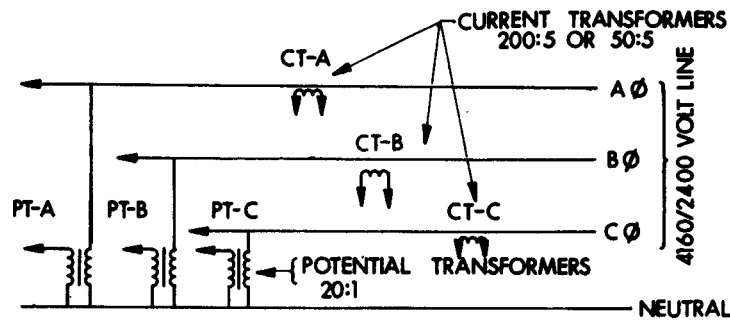
Load kW and kVARs
3-phase voltage
3-phase current.

This information is sampled at 5-second intervals and is available in either tabular or graphic form as required.

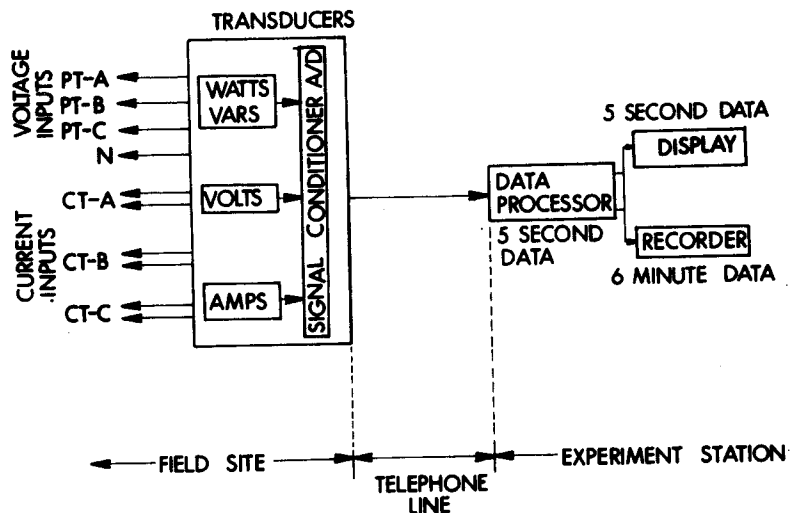
Figure 11 shows the electrical connection and Table VII shows full-scale and typical readings. The accuracy of the transducers was 1% and a 12-bit (4096 count) analog-to-digital converter was used. Five-second averages of the data were sent to the data processor at the NE RES where they were displayed, and 6-minute averages were computed and recorded. Only two phases of the 3-phase circuit are in use at the NE RES end of the CMLP circuit.

A week's recorded data was processed at one time, producing daily summary reports. Table VIII shows a typical report for the three sites on energy, VARs, power, power factor, voltage and current. These data are based on 6-minute averages; the maximums and minimums are the largest and smallest 6-minute average samples for the day. When there is a net power or energy flow from the NE RES to the utility line, it shows as a minus (-) kW or kWh. In

addition, 5-second data can be recorded for short periods so that fine-grain information can be tabulated and plotted. The 5-second recording capability permits observation of the effects of load changes before the voltage regulators can respond or other load changes obscure the observations.



(a)



(b)

Fig. 11. (a) Pole-top-mounted transformers for UDAC;
 (b) UDAC block diagram.

TABLE VII
SUMMARY OF UDAC INSTRUMENTATION CAPABILITIES

	Boston Edison Substation			CMLP Substation			CMLP RES end		
	Full	Scale	Typical	Full	Scale	Typical	Full	Scale	Typical
Power kW	3600		554	1200		775	300		70.2
VARs	3600		120	1200		144	300		8.2
Voltage A	3000		2246	3000		2442	3000		0.0*
B	3000		2460	3000		2441	3000		2367
C	3000		2430	3000		2448	3000		2397
Current A	600		77.3	200		119.3	50		0.0*
B	600		97.5	200		91.0	50		15.4
C	600		63.3	200		120.8	50		15.3

*
This phase is not used at the NE RES; the transformer primary fuse is removed.

TABLE VIII
DAILY SUMMARY FROM UDAC MEASUREMENTS

MEASURES DAILY REPORT: FRIDAY UTILITY POSITIONING RESULTS	5/28/82	LEXSB	CML17	CMRES
TOTAL ENERGY (KWH)	7075.56	14971.31	85.52	
TOTAL ENERGY DURING SUNHOURS (KWH)	4550.62	10286.48	48.61	
TOTAL REACTIVE ENERGY (KVAR-H)	2705.34	3178.47	79.95	
AVERAGE ECWEE (KW)	297.75	630.03	3.57	
MAXIMUM ECWEE (KW)	413.96	820.61	31.64	
MINIMUM ECWEE (KW)	173.14	402.54	-12.45	
AVERAGE REACTIVE ECWEE (KVAR)	113.85	133.76	3.34	
MAXIMUM REACTIVE ECWEE (KVAR)	138.87	249.03	15.01	
MINIMUM REACTIVE ECWEE (KVAR)	86.13	42.19	0.44	
AVERAGE ECWEE FACTOR	0.93	0.98	0.65	
MAXIMUM ECWEE FACTOR	0.97	0.99	1.00	
MINIMUM ECWEE FACTOR	0.86	0.95	-0.64	
AVERAGE VCITAGE - PHASE A (V)	2439.27	2443.78	0.0	
AVERAGE VCITAGE - PHASE B (V)	2458.85	2440.17	2415.34	
AVERAGE VCITAGE - PHASE C (V)	2433.60	2448.04	2472.12	
MAXIMUM VCITAGE - PHASE A (V)	2461.60	2472.59	0.0	
MAXIMUM VCITAGE - PHASE B (V)	2478.45	2466.00	2427.91	
MAXIMUM VCITAGE - PHASE C (V)	2452.81	2475.52	2496.76	
MINIMUM VCITAGE - PHASE B (V)	2424.25	2414.73	0.0	
MINIMUM VCITAGE - PHASE C (V)	2433.77	2412.53	2399.35	
MINIMUM VCITAGE - PHASE A (V)	2416.19	2417.66	2444.76	
AVERAGE CURRENT - PHASE A (A)	48.15	104.07	0.0	
AVERAGE CURRENT - PHASE B (A)	41.98	69.32	1.46	
AVERAGE CURRENT - PHASE C (A)	45.50	99.29	1.13	
MAXIMUM CURRENT - PHASE B (A)	73.97	144.82	0.0	
MAXIMUM CURRENT - PHASE C (A)	58.74	98.68	8.73	
MAXIMUM CURRENT - PHASE A (A)	67.53	127.44	4.58	
MINIMUM CURRENT - PHASE A (A)	26.07	65.67	0.0	
MINIMUM CURRENT - PHASE B (A)	22.70	41.70	0.07	
MINIMUM CURRENT - PHASE C (A)	31.64	64.75	0.13	
HOURS OF DATA RECORDED	23:45	23:45	23:57	

6.0 COMPARISON OF MODEL PREDICTIONS WITH MEASUREMENTS

6.1 Loading Tests at NE RES

As a check of the line-impedance values, voltage changes at the NE RES were measured while connecting and disconnecting a 25-kW, single-phase resistive load located in the Westinghouse prototype PV system. The calculated value of the voltage change at the end of the high-voltage feeder was obtained by a simple model, which used the value of Z_o of $0.189 + j.215$ ohms per 1000 feet, and the length of the feeder, which is about 15,500 feet to the NE RES (see Figs. 1 and 2). Using this approach, the calculated voltage change was 1.3%, or 1.54 V on a 120-V base. The calculated result from a computer model based on Fig. 2 was 1.25%, or 1.5 V. The measured voltage change ranged from 1.2 to 1.6 V, which is 1.0 to 1.3%. (This voltage change was observed using one of the 20:1 potential transformers which are described in the section on instrumentation, as shown in Fig. 11). The measured voltage change is in good agreement with the models, given the uncertainty in calculating the neutral conductor configuration.

It is interesting to note that the voltage changes observed at the 25-kW load's 240-V terminals were about 6 V, or 2.5%, as the load was switched on and off. This additional voltage change is due to the impedance of the 75-kVA distribution transformer and the 120/240-VAC secondary wiring to the load center in the prototype building. The voltage changes observed by the "customer" (in this case the 25-kW load) are about evenly divided between voltage changes occurring along the high-voltage primary and the voltage changes occurring in the transformer and secondary wiring.

It is important to note that the voltage changes observed in single-phase loads or PV injection will be about six times greater than if the same amount of load or PV injection were distributed over the three phases. This is because one-third of the load is on each phase in the three-phase connection. Further, since the load is balanced, voltage changes in the neutral conductor cancel, so the round-trip voltage change is approximately halved.

Although single-phase values were useful in checking operation at the NE RES, the feeder model was developed on a balanced three-phase basis. It

is expected that any significant level of PV generation would be spread over a sufficient area to be connected to all three phases or, in the case of a large concentrated installation, would be operated as a three-phase system.

A series of staged tests was made on 14 May 1982. The first test consisted of turning on and off about 82 kW of resistive load on the two phases at the NE RES location. The results are shown in Fig. 12. Note that results of measurements at the NE RES use the scale on the left side of the graphs and the measurements at the substation end, Pole 17, use the scale at the right side of the graphs. As expected, the change in kilowatts and amperes was quite visible at both source and load ends of the feeder, although the 18-ampere change is somewhat dwarfed by the 140 amperes already on the feeder. The changes are most apparent at the NE RES end of the line. The voltage change of 1.5 to 2% at the load end was not visible at the source end.

6.2 PV Injection from the NE RES

Another set of tests (see Fig. 13) was made to determine the effect of intermittent injection of solar power into the feeder. About 15 kW of PV generation was switched on and off, and the effects were noted. While the power level change was quite apparent at the NE RES, it was not visible in the total feeder load at Pole 17. Nor was the 4-ampere current change visible in the context of a variable 130-ampere feeder load. No effect on voltage was visible at either end. It appears that observation of the small amount of injected power must be made at a time when fewer load changes are occurring on the feeder. The inverter power factor of two of the four inverters is in the range of 0.7 to 0.8, and it was shown previously that little voltage change results with inverter power factors in this range. The other two inverters are near unity power factor.

One potential use of these tests is to validate the model calculations. It was not feasible, however, to obtain better correlation without knowing the exact position and effect of the line regulators. Calculated total drops of 8% from Pole 17 to the end can only be checked against measured drops of 2% if the amount of regulator boost at the time is known. Some means of monitoring or locking the regulators for a period is necessary in order to correlate these results.

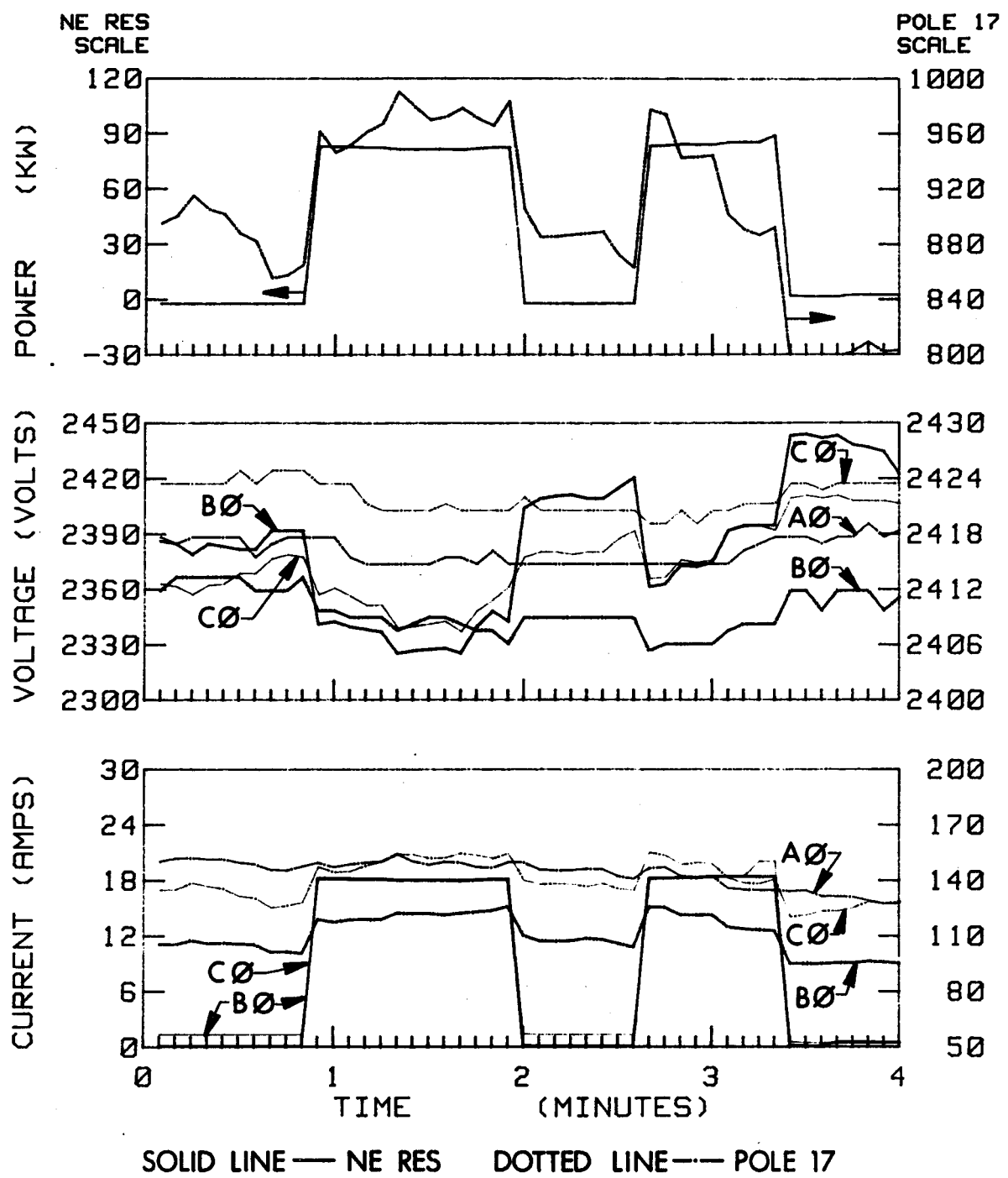


Fig. 12. Feeder measurements with switched loads at the NE RES.

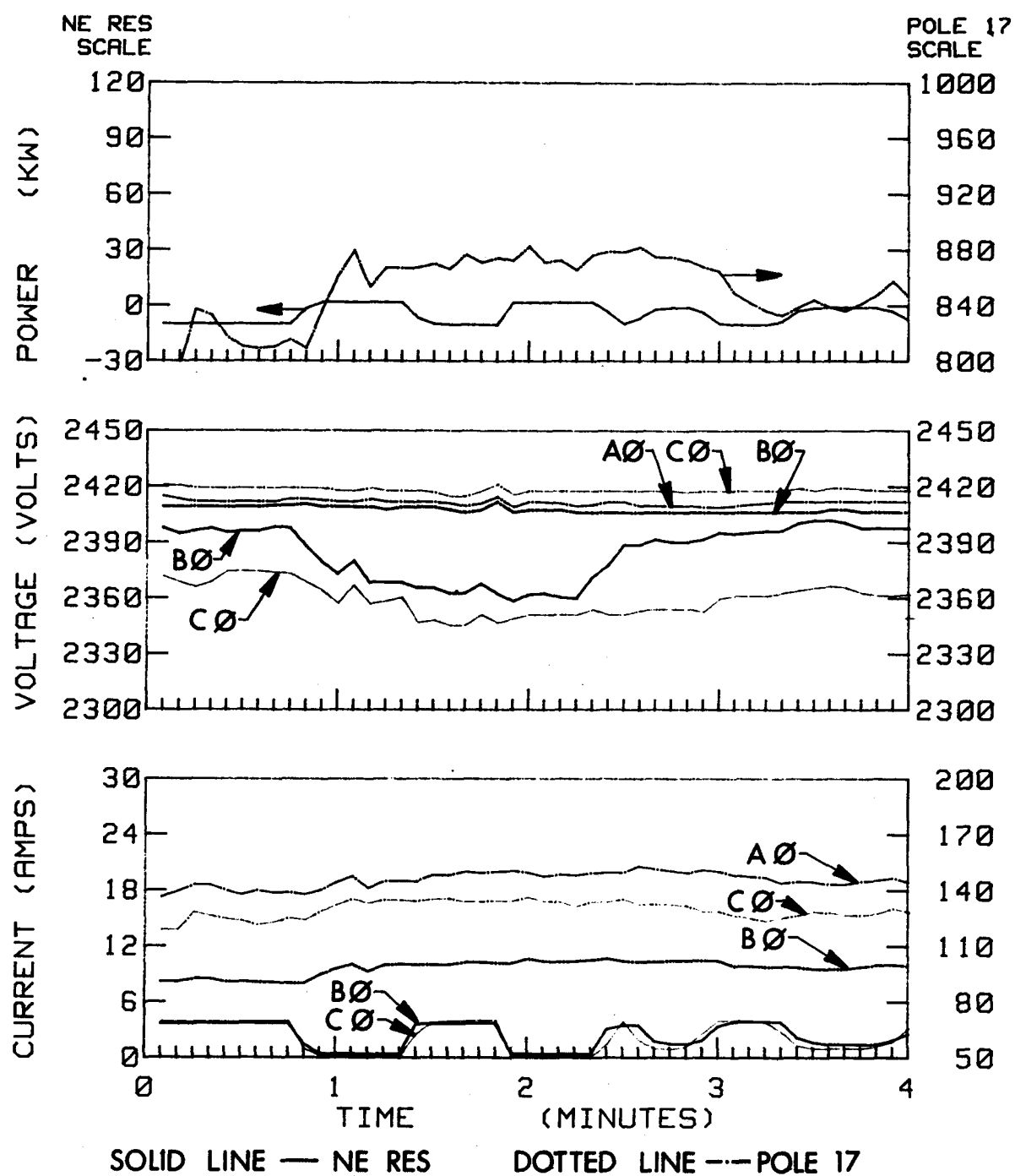


Fig. 13. Feeder measurements with PV-generated power injected at the NE RES.

7.0 MEASUREMENT OF AMBIENT HARMONIC VOLTAGES AND CURRENTS

Field tests made on 14 May 1982 at Pole 17 on the CMLP feeder, shown in Fig. 14, include oscillograms of existing currents on the feeder. Table IX gives the harmonic analysis of these curves. It was noted that the feeder is already carrying 3rd and 5th harmonic currents of about 5 amperes each near its source. These harmonic currents are a natural result of the non-linear magnetizing characteristics of distribution transformer cores. They are known to be prevalent on distribution systems, and to fluctuate with variations in voltage.

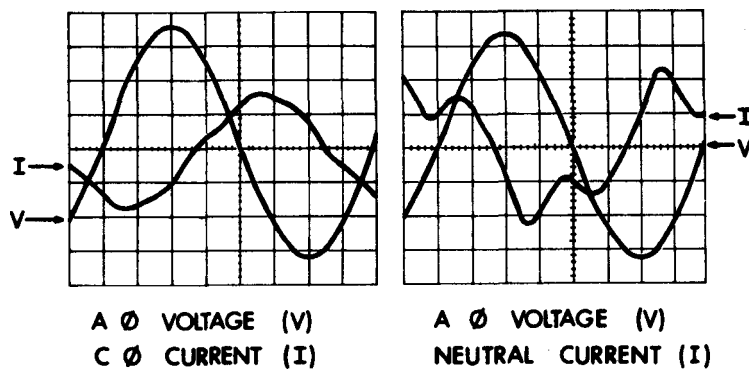


Fig. 14. Voltage and current waveforms measured on CMLP Circuit 23 at Pole 17 (near substation).

TABLE IX
HARMONICS MEASURED ON CMLP CIRCUIT 23 AT POLE 17
(May 14, 1982 between 2 and 4 p.m.)

Harmonic Content in Percent of Fundamental

Parameter Measured	Harmonic										
	2	3	4	5	6	7	8	9	10	11	
A-Phase Voltage	0	0.7	0	1.3	0	0.25	0	0	0	0	
A-Phase Current	0.15	3.0	0.1	3.0	0	0.4	0	0.3	0	0	
C-Phase Current	0.2	3.4	0	3.4	0	0.1	0.2	0.1	0	0.1	
Neutral Current*	1.6	50.0	0.3	14.1	0.7	3.2	0.3	--	--	--	

* Due to the three-phase balance of loads, the fundamental component of neutral current is about 10% of any individual phase current.

It is interesting to note that the 3rd harmonic currents, which in this case comprise only about 3% of the fundamental on each phase, add together to form about 50% of the neutral current.* These odd harmonics flow back to the substation power transformer where they are dissipated in the delta-connected winding of the transformer. Since a delta-connected power transformer provides a virtual short circuit for odd harmonic currents, the harmonic currents seldom create much of a problem, even though they are present in substantial quantities.

It is not expected that the small increase in harmonic current resulting from 500 kW of solar inverters will present any substantial increase in the problem. We do not presently know enough about the time/phase relationship of the harmonics to be certain of whether the inverter harmonics will add to or subtract from the already existing harmonic currents. Resonances with tuned loads are already a fairly familiar problem and can be dealt with by various means, such as traps, choke coils, capacitors or load relocation.

*Neutral current can be measured using the current transformers shown in Fig. 11(a) by looping three of the current transformer secondaries through a clamp-on current probe. The resulting flux sensed is proportional to the neutral current. (It is necessary to observe the polarity convention of the current transformers when connecting the probe.)

8.0 CONCLUSIONS

We have examined the criteria which a distribution engineer would normally review in determining the viability of a new load. These criteria include feeder loading, voltage drop and flicker, and harmonic distortion of the waveform. Addition of PV-power sources is not expected to result in any problem which cannot be dealt with by readily available means. These methods can easily be applied to other feeders which are candidates for significant amounts of PV generation. Feeder-conductor thermal loading and losses will be reduced substantially. Loss reduction on a heavily loaded feeder, such as the one studied, is significant and can result in a substantial bonus (as much as 30%) in terms of kW and kWh savings to the utility.

Voltage fluctuations due to changes in insolation level will not be excessive at levels of PV penetration up to 25% of peak load.

Harmonic distortion was examined both from the viewpoint of the ability of the line capacitors to tolerate the harmonic currents imposed, and the ability of customers' equipment to tolerate the harmonic content of the voltage waveform produced. Both criteria appear to be satisfactory even with a "worst-case" inverter with considerable harmonics in the output current waveform.

We would further comment that for reasons of voltage stability, inverters which operate near 0.85 power factor are not necessarily detrimental to the utility either from the standpoint of voltage regulation or line losses. The VAR demand of these units, however, would need to be met in a suitable fashion.

This study has shown that even with relatively large penetrations (approximately 25% of peak load), PV utility-interactive sources will not be detrimental to the operation of a utility.

REFERENCES

1. Draft, Committee Report, "IEEE Position Paper on Dispersed Storage and Generation," June 10, 1981, IEEE Power Engineering Society Summer Meeting, 1981.
2. H. A. Fenton, C. H. Much, "Residential Photovoltaic Experiment Station Data System," MIT Lincoln Laboratory Technical Report, November 1981, DOE/ET/20279-155.
3. General Electric Co., "Distribution Data Book," GET 1008M, July 1980.
4. J. Fitzer, et al, "Impact of Residential Utility Interactive PV Power Systems on the Utility," prepared by the University of Texas at Arlington under contract to MIT Lincoln Laboratory, September 1982, DOE/ET/20279-222.
5. V. Del Toro, Principles of Electrical Engineering, Chapter 5, Prentice-Hall, New York, 1965.
6. G. L. Campen, "An Analysis of the Harmonics and Power Factor Effects of a Utility Intertied Photovoltaic System," IEEE 82-SM-328-3, IEEE Power Engineering Society Summer Meeting, San Francisco, 18-23 July 1982.
7. E. E. Landsman, "Analysis and Test of Line-Commutated Inverters for use in Residential Photovoltaic Power Systems," MIT Lincoln Laboratory Technical Report, May 1980, DOE/ET/20279-127.
8. Electrical Transmission and Distribution Reference Book, 4th Edition, by Central Station Engineers of Westinghouse Electric Corp., Chapter 8, E. Pittsburgh, PA, 1950.

ACKNOWLEDGMENT

The authors wish to thank the staff of the Concord Municipal Light Plant for their cooperation in the performance of this study.

APPENDIX A
LINE LOSSES VERSUS LOAD AND PV INJECTION

TABLE A1
LINE LOSS REDUCTION WITH PV GENERATION AT NE RES
MEDIUM LOAD ON CMLP CIRCUIT 23

Condition	$\Delta P_{\text{substation}}$ in kW	$P_{\text{substation}}$ in kW	Line Losses in kW	Line Losses as % of total load	Δ Line Loss in kW	P_{solar} in kW	Solar Bonus in %*
No PV generation:	1643.76	--	127	8.3	--	0	--
50-kW PV generation:							
PF = 1.0	1582.30	61	115	7.9	11	50	23
50-kW PV generation:							
PF = 0.85	1586.26	58	119	8.1	7	50	15

LIGHT LOAD ON CMLP CIRCUIT 23

No PV generation	884.93	--	38	4.4	--	0	--
200-kW PV generation:							
PF = 0.85	672.76	212	26	3.0	12	200	6

* Solar Bonus is defined in Table II in the report.

TABLE A2
 LINE LOSS REDUCTION WITH UNIFORMLY DISTRIBUTED PV
 GENERATION ON TESCO FEEDER 7.2/12.5 kV
 (31 July 1980; 2 p.m.)
 (Data from Reference 4)

Condition	$P_{\text{substation}}$ in kW	$\Delta P_{\text{substation}}$ in kW	Line Losses in kW	Line Losses as % of total load	Δ Line Loss in kW	P_{solar} in kW	Solar Bonus in %
No PV generation:	6603	--	147	2.3	--	--	--
40% of customers have PV generation:							
PF = 1.0	3562	3041	50	.8	97	2944	3.3
PF = 0.85	3565	3038	55	.9	92	2946	3.1
PF = 0.7	3569	3024	69	1.0	78	2946	2.7
80% of customers have PV generation:							
PF = 1.0	579	6024	11	.2	136	5888	2.3
PF = 0.85	605	5998	41	.6	106	5892	1.8
PF = 0.7	666	5937	106	.6	41	5896	0.7

TABLE A3

LINE LOSS REDUCTION FOR CONCENTRATED PV
GENERATION ON TESCO 7.2/12.5 kV FEEDER(31 July 1980; 2 p.m.)
Data from Reference 4

Condition	$P_{\text{substation}}$ in kW	$\Delta P_{\text{substation}}$ in kW	Line Losses in kW	Line Losses as % of total load	Δ Line Loss in kW	P_{solar} in kW	Solar Bonus in %
No PV generation	6603	--	147	2.3	--	--	--
40% PV generation concentrated at end of feeder:							
PF = 1.0	3890	2713	43	0.6	104	2609	4.0
PF = 0.85	3898	2705	52	0.8	95	2610	3.6
PF = 0.70	3922	2681	77	1.2	70	2611	2.7
20% PV generation concentrated at end of feeder:							
PF = 1.0	5111	1492	84	1.3	63	1429	4.4
PF = 0.85	5116	1487	85	1.3	62	1425	4.3
PF = 0.70	5126	1477	93	1.4	54	1423	3.8